Two physically, functionally, and developmentally distinct peritoneal macrophage subsets

Eliver Eid Bou Ghosn[a,b,1], Alexandra A. Cassado[c], Gregory R. Govoni[d], Takeshi Fukuhara[a], Yang Yang[a], Denise M. Monack[d], Karina R. Bortoluci[c,e], Sandro R. Almeida[b], Leonard A. Herzenberg[a], and Leonore A. Herzenberg[a]

[a]Department of Genetics, Stanford University School of Medicine, Stanford, CA 94305; [b]Department of Clinical Analysis, Faculty of Pharmaceutical Sciences, [c]Department of Immunology, Institute of Biological Sciences - ICB IV, Universidade de São Paulo, São Paulo SP 05588, Brazil; [d]Department of Microbiology and Immunology, Stanford University School of Medicine, Stanford, CA 94305; and [e]Department of Biological Sciences, Universidade Federal de São Paulo, Diadema SP 09972, Brazil

Contributed by Leonard A. Herzenberg, December 28, 2009 (sent for review December 12, 2009)

The peritoneal cavity (PerC) is a unique compartment within which a variety of immune cells reside, and from which macrophages (MØ) are commonly drawn for functional studies. Here we define two MØ subsets that coexist in PerC in adult mice. One, provisionally called the large peritoneal MØ (LPM), contains approximately 90% of the PerC MØ in unstimulated animals but disappears rapidly from PerC following lipopolysaccharide (LPS) or thioglycolate stimulation. These cells express high levels of the canonical MØ surface markers, CD11b and F4/80. The second subset, referred to as small peritoneal MØ (SPM), expresses substantially lower levels of CD11b and F4/80 but expresses high levels of MHC-II, which is not expressed on LPM. SPM, which predominates in PerC after LPS or thioglycolate stimulation, does not derive from LPM. Instead, it derives from blood monocytes that rapidly enter the PerC after stimulation and differentiate to mature SPM within 2 to 4 d. Both subsets show clear phagocytic activity and both produce nitric oxide (NO) in response to LPS stimulation in vivo. However, their responses to LPS show key differences: in vitro, LPS stimulates LPM, but not SPM, to produce NO; in vivo, LPS stimulates both subsets to produce NO, albeit with different response patterns. These findings extend current models of MØ heterogeneity and shed new light on PerC MØ diversity, development, and function. Thus, they introduce a new context for interpreting (and reinterpreting) data from ex vivo studies with PerC MØ.

CD11b | F4/80 | lipopolysaccharide | peritoneal cavity | thioglycolate

The mouse peritoneal cavity (PerC) selectively attracts and maintains specialized immune cells, including the PerC macrophages (MØ) that are our principal focus here. MØ are typically characterized as large cells that express surface F4/80 glycoprotein and CD11b, one of the chains of the Mac-1 integrin (1–3). Initially thought to be a single subset represented in blood as monocytes and in tissues as differentiated "resident MØ" (4, 5), several MØ subsets have now been recognized based on morphological, functional, and phenotypic differences (2, 6, 7). In addition, two subsets of functionally distinct blood monocytes have been described (8, 9).

Much of current fundamental knowledge about MØ biology comes from analysis of cells drawn from mouse PerC, which became widely used as a MØ source as a result of pioneering work by Cohn and collaborators in the 1960s (10). However, although MØ populations present elsewhere in the animal have recently been shown to be functionally and phenotypically heterogeneous, virtually no attention has yet been paid to potential heterogeneity among PerC MØ (2, 9, 11).

Here, we distinguish two coexisting PerC MØ subsets and show that these have unique phenotypic, functional, and developmental characteristics. Based on the size differences that we detect between these subsets, we provisionally refer to them as small peritoneal MØ (SPMs) and large peritoneal MØ s (LPMs).

Both SPMs and LPMs express the typical F4/80 and CD11b MØ surface markers and both show clear phagocytic activity in vivo. However, they differ sharply in their expression of a wide variety of surface molecules, including Gr-1 and MHC-II, and show strikingly different response patterns to stimulation with typical MØ stimuli [e.g., lipopolysaccharide (LPS), thioglycolate]. Furthermore, they are developmentally independent. LPMs, which rapidly disappear from PerC following LPS or thioglycolate stimulation, do not give rise to SPMs, which increase in numbers at this time. Instead, SPMs derive from blood monocytes that migrate into the PerC in large numbers in response to the stimulation.

Thus, we show here that a source traditionally used to obtain MØ for functional studies actually yields two highly distinct types of MØ. We discuss these findings in the context of current views of MØ origins and functions, and tentatively locate at least one of these PerC subsets (i.e., SPMs) in an extended model based on the framework introduced by Geissmann et al. (9) for blood and tissue MØ.

Results

Mouse PerC Contains a Variety of Immune Cells from the Lymphoid and Myeloid Lineages. To identify the immune cell subsets present in the mouse PerC, we used high-dimensional flow cytometry (i.e., FACS) with stain sets capable of distinguishing as many as 11 markers per cell. We collected data for single live PerC cells from untreated BALB/c adult mice and gated to reveal the following subsets (Fig. 1): B cells, MØ, dendritic cells (DCs), eosinophils, mast cells, neutrophils, T cells, natural killer cells, and invariant natural killer T cells.

Approximately 40% of the PerC cells are B-lymphocytes ($CD19^+$; Fig. 1, second row). Among the remaining "non-B" PerC cells, the majority coexpress CD11b and F4/80 and hence are appropriately characterized as MØ. Among these, we find the two unique MØ subsets that are the principal focus of this manuscript.

Peritoneal MØ Are Composed of Two Distinct Subsets: SPMs and LPMs. Within the $CD11b^{hi}$ population (gated as in Fig. 1), we find two subsets that differ strikingly in size, surface marker phenotype, and function. Based on size differences determined by FACS scatter profiles and microscopy images (Fig. 2 *A* and *B*), we provisionally refer to these subsets as SPMs and LPMs. LPM is the most abundant MØ subset (approximately 90% of PerC MØ) in unstimulated mice; SPM accounts for the remaining 10% of the PerC MØ (Fig. 1, last panel).

Author contributions: E.E.G. and L.eonore A. Herzenberg designed research; E.E.G. and A.A.C. performed research; G.R.G, T.F., and D.M.M. contributed new reagents/analytic tools; E.E.G., A.A.C., G.R.G., T.F., Y.Y., D.M.M., K.R.B., S.R.A., Leonard A. Herzenberg, and Leonore A. Herzenberg analyzed data; and E.E.G., K.R.B., and Leonore A. Herzenberg wrote the paper.

The authors declare no conflict of interest.

[1]To whom correspondence should be addressed. E-mail: eliverg@stanford.edu.

This article contains supporting information online at www.pnas.org/cgi/content/full/0915000107/DCSupplemental.

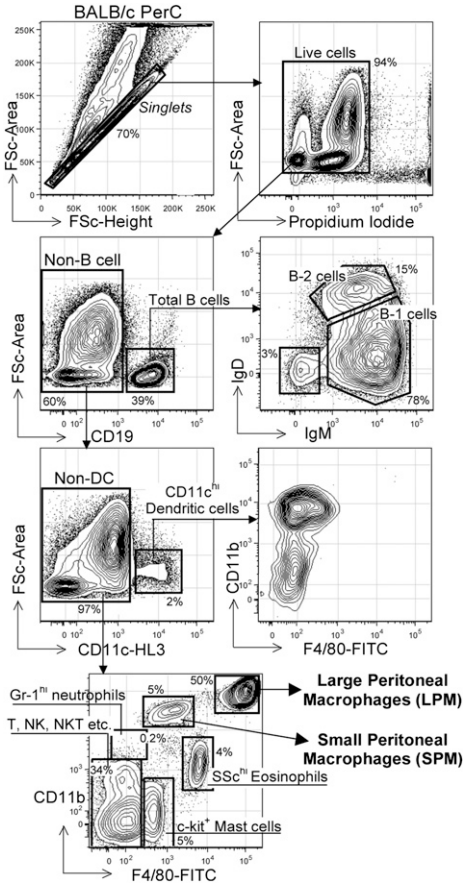

Fig. 1. Naive mouse PerC contains a variety of immune cell subsets. Gating strategy used to identify immune cells present in PerC based on surface molecules. Total PerC cells from unstimulated BALB/c mice were processed and analyzed as described in *Materials and Methods*. Data shown are representative of >10 experiments.

The expression of a series of surface markers clearly distinguishes SPM from LPM (Table 1). Both subsets express the prototypical MØ markers CD11b and F4/80. However, LPM expresses approximately three times as much CD11b and approximately 80 times as much F4/80 as SPM, setting the two subsets apart from each other and from other PerC cells (Fig. 1 and Table 1).

Importantly, the expression of three additional surface markers qualitatively distinguishes SPMs from LPMs. Thus, LPMs express Gr-1 and AA4.1 whereas SPMs do not (Table 1). In contrast, SPMs express MHC- II (I-A) whereas LPM strikingly do not express this classical marker, measured by FACS analyses (Table 1).

The quantitative expression of a series of other well known surface markers also distinguishes SPMs from LPMs (Table 1). Notably, CD40, CD80, CD86, CD11c (N418 MAb), and TLR4 are all expressed at higher levels on LPMs than SPMs.

Eosinophils, which are commonly found in PerC, will contaminate the SPM and LPM compartments unless explicitly excluded by the gating strategy. The eosinophils express F4/80 at a level intermediate between SPM and LPM (Fig. 1, last panel). However, they can be excluded because they characteristically express low levels of CD11b and low to intermediate levels of Gr-1, and have a unique scatter profile ($CD11b^{low}$, $Gr\text{-}1^{int}$, and SSc^{hi}; Figs. 1 and 3 and Fig. S1). Therefore, we standardly use a gating strategy that excludes these cells from the SPM and LPM subsets. Importantly, these data strongly argue against the common practice of using either F4/80 or CD11b as the sole surface marker for identifying or isolating MØ.

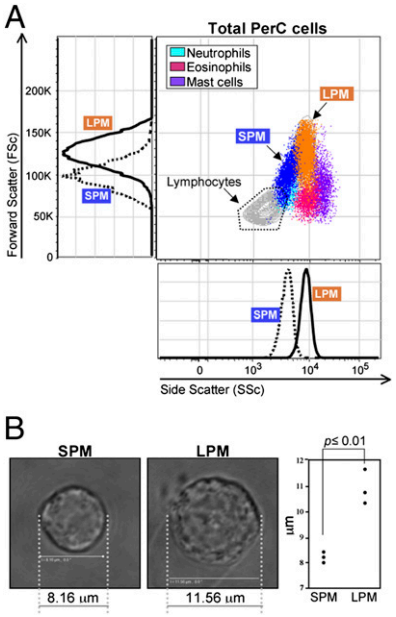

Fig. 2. The two distinct PerC MØ subsets are differentiated by size. (*A*) PerC MØ (and other cell types) were analyzed for their scatter profile (forward and side: size and granularity, respectively) by flow cytometry. (*B*) SPMs and LPMs were FACS-sorted and their diameter were measured. Representative differential interference contrast images are shown.

SPMs and LPMs Are Distinct from DCs and Monocytes. DCs in PerC and spleen are smaller than either SPMs or LPMs and do not express CD11b and F4/80 at the levels found on SPMs and LPMs (Fig. 1, third row). In addition, PerC and splenic DCs both

Table 1. Distinct phenotypic profile of SPMs and LPMs

Surface molecule	SPMs	LPMs	PerC DC	Spleen DC
MHC-II (I-A)	60,000	NS	–	–
Gr-1	NS	6,000	–	–
Ly-6C	NS	NS	–	–
MHC-I (H-2K)	1,600	800	–	–
CD11b	24,000	84,000	–	–
F4/80	1,200	97,000	–	–
AA4.1	NS	12,000	–	–
TLR4	80	540	–	–
TLR4 after in vivo LPS	130	340	–	–
c-kit	NS	NS	–	–
DX5	NS	NS	–	–
CD40	160	600	–	–
CD80	700	3,700	–	–
CD86	140	1,700	–	–
HL3 MAb (CD11c)	300	NS	9,000	33,500
N418 MAb (CD11c)	500	2,900	4,000	10,000

PerC cells from unstimulated BALB/c were harvested and stained and both SPMs and LPMs were analyzed for the expression of several surface markers. SPMs, LPMs, and PerC DsC were identified as in Fig. 1. Spleen DCs were identified as $CD11c^{hi}$, $MHC\text{-}II^{hi}$, and Lin^{-}. Values are displayed as MFI. The value for the expression of each surface marker was obtained by subtracting the MFI of the full stained cells from the MFI of fluorescence-minus-one control (18, 19). Cells that expressed MFI for a given marker similar or equal to fluorescence-minus-one control were considered negative for this marker and hence were annotated as NS. Data shown are representative of more than five experiments. NS, not significant.

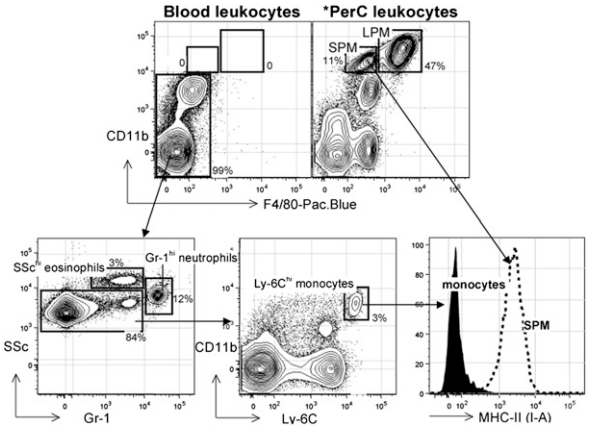

Fig. 3. SPMs and LPMs are absent in mouse blood. PerC and blood cells from unstimulated BALB/c mice were stained and analyzed for specific surface markers. *SPM and LPM were identified as in Fig. 1; blood monocytes were identified as Ly-6C^{hi}, CD11b^{+} cells. SPMs and LPMs are also absent in other naive lymphoid organs, such as spleen and lymph nodes (Fig. S2).

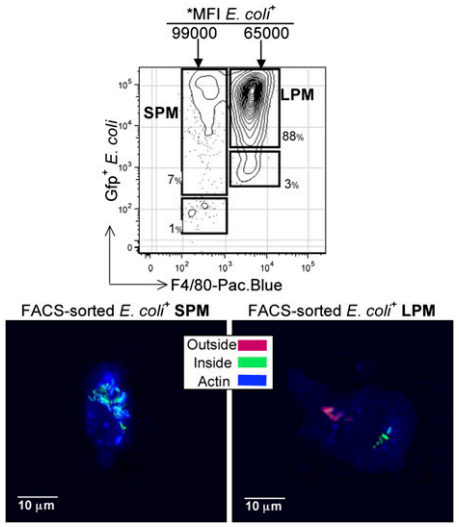

Fig. 4. Both SPMs and LPMs are able to phagocyte bacteria in vivo. *E. coli* (5×10^6) expressing GFP were injected i.p. into BALB/c mice and, after 2 h, PerC cells were harvested and stained as described in *Materials and Methods*. Flow cytometry analysis reveals that most SPMs and LPMs were positive for GFP, indicating that they had internalized bacteria. Confocal images: GFP^{+} SPMs and LPMs were FACS-sorted and analyzed to confirm whether the bacteria had been internalized: green, internalized *E. coli*; blue, actin (phalloidin); red, anti-LPS (red staining indicates that bacteria have remained adherent to the outer cell membrane, i.e., not phagocytized).

express high levels of CD11c, although PerC DCs have only approximately half as much CD11c as splenic DCs (Table 1). SPMs and LPMs, in contrast, express much less CD11c. This difference is detectable when CD11c is revealed by either HL3 or N418 monoclonal anti CD11c. Interestingly, staining with the monoclonal HL3 detects very little (if any) CD11c on LPMs whereas staining with the monoclonal N418 reveals somewhat more CD11c on LPMs than SPMs (Table 1).

Monocytes differ from SPMs and LPMs with respect to phenotype and principal location. Monocytes are present in blood (Fig. 3) and migrate to tissues to become resident MØ (8, 9). In contrast, neither SPMs nor LPMs are detectable in blood (Fig. 3), and these cells are virtually absent in spleen and lymph nodes (Fig. S2). We note, however, that the L-selectin CD62L is expressed on approximately half of SPMs in PerC (Fig. S3), suggesting that, with appropriate stimulation, SPMs may be able to migrate to lymphoid organs.

Phenotypically, SPMs and LPMs are clearly distinct from monocytes. CD11b expression is markedly higher on both SPM and LPM than it is on monocytes, and indeed on all blood leukocytes (Fig. 3). In contrast, Ly-6C is not detectable on SPMs or LPMs but is very high on monocytes (8, 9) (confirmed in Fig. 3). F4/80 expression on SPMs and LPMs also distinguishes these cells from blood leukocytes (Fig. 3), even though the F4/80 levels on SPMs are only a little above background.

SPM and LPM Are Present in All Mouse Strains Tested. SPMs and LPMs are detectable in PerC from all of the strains analyzed in this study, including BALB/c, C57BL/6, 129/S6, FVB/N, SJL/J, and RAG$^{-/-}$ (Fig. S4). The relatively constant frequencies of these subsets in PerC, and their similar proportionality among non-B PerC leukocytes suggests that there may be an evolutionary advantage to maintenance of the composition of the apparently free-living peritoneal leukocytes.

SPM and LPM Are Functionally Distinct. ***Phagocytosis.*** MØ are essential for host protection against infections, in large part because their unique ability to ingest and degrade microorganisms. SPMs and LPMs both have this ability, albeit with somewhat different characteristics. To measure phagocytosis by these cells, we used an in vivo phagocytosis assay in which live GFP-expressing (i.e., fluorescent) *Escherichia coli* were injected intraperitoneally and PerC cells were harvested 2 h later. The harvested cells were immediately chilled, centrifuged to eliminate free bacteria, stained for surface markers, and then analyzed by flow cytometry to determine whether GFP^{+} bacteria were present in SPMs and LPMs.

Findings demonstrate that both SPMs and LPMs phagocytize substantial numbers of GFP^{+} bacteria within 2 h (Fig. 4). These two subsets account for most of the phagocytosis that occurs in PerC, at least among the cells that are free to be harvested from the PerC. Confocal microscopy of sorted GFP^{+} cells confirms that the bacteria are localized inside the cells (rather than adherent to the surface) and hence that they are indeed phagocytized (Fig. 4).

FACS analyses show that there are more bacteria in SPM than LPM. However, quantitative interpretation of these data are difficult because the GFP MFI only reports the presence of intact, and most likely still living, bacteria. Thus, although we find that SPMs have higher bacterial loads (i.e., GFP fluorescence) by this measure than LPMs [99,000 vs. 65,000 GFP median fluorescence intensity (MFI), respectively], we do not know whether this is a result of more efficient phagocytosis by SPMs or more efficient killing of phagocytized bacteria by LPMs. In any event, these phagocytosis studies (Fig. 4) reveal dramatic differences in the way that SPMs and LPMs relate to peritoneal infection.

NO production. MØ are well known to express Toll-like receptor (TLR) and other specialized receptors that can trigger responses to soluble products derived from microorganisms (3). TLR4, which triggers responses to bacterial LPS, is readily detectable on LPMs harvested from unstimulated animals. However, it is only minimally above background on SPMs (Table 1).

Consistent with this finding, ex vivo LPS stimulation for 20 h triggers PerC LPMs to produce large amounts of NO but does not trigger detectable NO production by SPMs in the same culture (Fig. 5*A*).

In vivo, LPS stimulation yields quite different results. It triggers strong NO production by both SPMs and LPMs and, in fact, stimulates more NO production by SPMs than LPMs (4,500 vs. 2,600 NO MFI, respectively; Fig. 5*B*). Further, LPS stimulation results in a modest decrease in TLR4 on LPM by 20 h after stimulation and a modest increase in TLR4 on SPM at this time (Table 1).

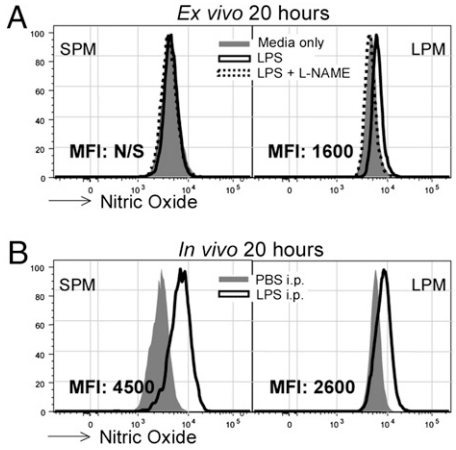

Fig. 5. SPMs and LPMs respond differently to TLR agonists. (*A*) PerC cells (10^6) were incubated with or without 1 μg/mL of LPS for 20 h at physiologic oxygen levels (5% O_2). The specificity of the NO measurement was confirmed by adding 1.5 mM L-NAME reagent into the culture, which specifically inhibits NO formation. (*B*) BALB/c mice were injected i.p. with 5 μg of LPS (or PBS solution control) for 20 h. SPMs and LPMs were identified as in Fig. 1 and Fig. S1. NO production was measured by flow cytometry using DAF-FM diacetate. N/S, not significant. For additional control data, see Fig. S5.

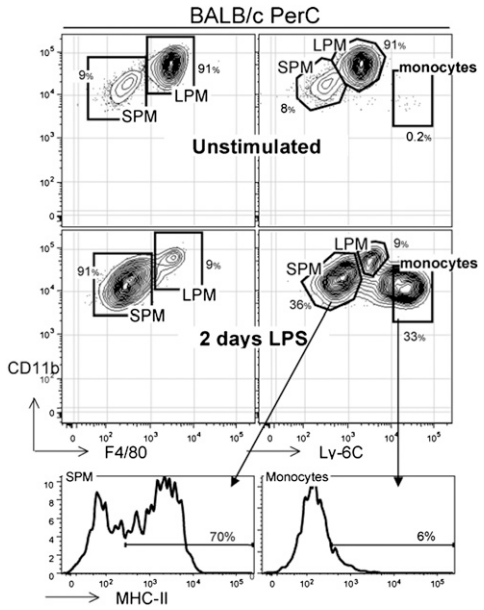

Fig. 6. LPS induces a dramatic shift in the SPM:LPM ratio. BALB/c were injected i.p. with 10 μg of LPS. After 2 d, PerC cells were harvested, stained, and analyzed for the presence of myeloid cells. SPMs and LPMs were identified as described in Fig. 1. Neutrophils and eosinophils were best gated out from this analysis by using the gating strategy shown in Fig. S1.

Collectively, these findings show that LPM produces as much or more NO in response to LPS in vitro as it does in vivo, whereas SPM fails entirely to produce NO in response to LPS in vitro but produces large amounts of NO in response to stimulation with this microbial product in vivo. Thus, whether responses to LPS are compared in vitro or in vivo, SPMs and LPMs behave differently in response to the same stimulus administered in the same environment.

Origins of the SPM Subset. Studies described in the previous section were conducted at 20 h after i.p. LPS injection because, at this time, PerC SPM and LPM frequencies are still comparable to the frequencies in unstimulated mice. However, by 2 d after stimulation, SPM becomes the dominant PerC MØ subset and LPM frequencies dwindle to less than 10% (Fig. 6). The most dramatic shifts occur in mice stimulated with higher doses of LPS (≥10 μg).

To determine whether this shift occurs because LPMs differentiate to SPMs, we sorted LPMs, labeled the sorted cells with CFDA-SE, and transferred them into PerC of unstimulated mice. One hour later, we stimulated the recipient mice with LPS and, at various times thereafter, we harvested PerC and determined the phenotype of the CFDA-SE^+ cells.

Results from these studies showed that, whether tested at 9 h or 2 d after stimulation, the sorted LPM population retains its LPM phenotype (Fig. 7). No CFDA-SE^+ cells appear in the SPM compartment, despite the virtual loss of the resident and the injected LPM cells by 2 d after stimulation. Thus, we conclude that LPS stimulation does not induce LPMs to differentiate to SPMs, and hence that LPM differentiation does not account for the increase in SPM frequency.

In contrast, examination of host PerC cells shows clearly that LPS stimulation induces a massive influx of cells that initially express the phenotype of the circulating monocytes in blood (Ly-$6C^{hi}$MHC-II^-). With time, the phenotype expressed by this large population of "monocytes" shifts toward the typical Ly-$6C^-$MHC-II^{hi} SPM phenotype (Fig. 6). Thus, our findings indicate that a wave of blood monocytes enters the PerC shortly after LPS stimulation and, over time, differentiates to SPMs.

Thioglycolate-Elicited MØ. Intraperitoneal injection of thioglycolate is widely used to enrich the yield of so-called activated PerC MØ, which are commonly collected 4 d after thioglycolate stimulation for use in functional MØ assays (12–14). Examination of PerC harvested from thioglycolate-stimulated animals at this time shows a shift in SPM and LPM frequencies similar to that induced by LPS (Fig. 8). LPM, normally the dominant PerC MØ subset, is

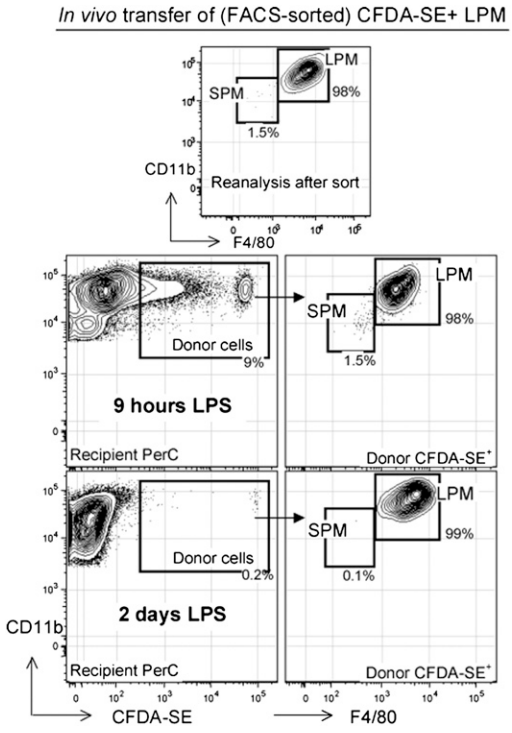

Fig. 7. SPMs are developmentally independent from LPMs. FACS-sorted and CFDA-SE-labeled LPMs (2×10^5) were injected i.p. into BALB/c recipients. Recipient mice were injected i.p. with LPS and, after 9 h or 2 d, PerC cells were harvested and stained and donor (CFDA-SE^+) cells were analyzed for surface phenotype.

barely detectable (<5% of total MØ). Thus, 4 d after thioglycolate stimulation, the myeloid population in PerC mainly contains SPM (FSc^{low}, CD11b^{int}, F4/80^{low}, Ly-6C^{-}, Gr-1^{-}). However, it also contains a small subset of monocytes (Ly-6C^{hi}) that most likely have infiltrated from blood (Fig. 8).

In addition, as in the response to LPS stimulation, we find that the monocyte population in thioglycolate-stimulated PerC shifts with time toward expression of the SPM phenotype. From d 1 onward, the "monocytes" in the thioglycolate-stimulated PerC show decreasing levels of Ly-6C and, somewhat later, increasing levels of MHC-II. By d 4, SPMs predominate with only a small percentage of cells expressing a typical monocyte phenotype (Fig. 8).

Overall, these findings indicate that results from studies with thioglycolate-elicited MØ may mainly reflect the behavior of SPMs and of monocytes that have recently developed into SPMs. However, it is important to recognize that, in addition to MØ, and regardless of harvest day, thioglycolate-stimulated PerC commonly contains additional subsets of immune cells that may participate in the responses being measured. Notably, on d 1 after stimulation, neutrophils can outnumber MØ and lymphocytes. Further, even on d 4, lymphocytes and granulocytes can be present in relatively large numbers (Fig. S1) and can complicate interpretation of findings putatively as a result of the activity of thioglycolate-elicited PerC "macrophages."

Discussion

Phenotypic and functional evidence presented here demonstrates that there are two distinct subsets of MØ in the mouse PerC. We provisionally refer to these subsets as SPMs and LPMs, as they differ in size as determined either by visual observation or by flow cytometric light-scatter measurements. Both subsets phagocytize bacteria in vivo (Fig. 4), and both express the canonical F4/80 and CD11b MØ markers (Fig. 1). However, as we have shown, they differ both qualitatively and quantitatively with respect to expression of several surface markers, including a key difference in the expression of MHC-II, which is expressed by SPMs but not LPMs (Table 1).

In addition, and perhaps most importantly from the standpoint of interpretation of functional data from studies with peritoneal MØ, SPMs and LPMs differ markedly in both their in vitro and in vivo responses to inflammatory stimuli (i.e., LPS or thioglycolate). In vitro, LPS induces LPMs to produce high levels of intracellular NO but fails to induce NO production by SPMs (Fig. 5*A*), even though the SPMs and LPMs are coharvested, cocultured, and costimulated in the same vessel. In vivo, in contrast, LPS stimulates NO production by both LPMs and SPMs, and in fact stimulates more NO production by SPMs than by LPMs (Fig. 5*B*).

Thus, our findings demonstrate that LPMs can respond to stimulation with microbial products presented either in vitro or in vivo. However, SPMs can respond only in a supportive environment, either because these cells are selectively sensitive to an inhibitor encountered in the culture or, more likely, because they require an additional stimulus/signal provided by the in vivo environment.

In principle, the production of NO by SPMs and LPMs should provide a basis for classifying these MØ subsets within the M1 and M2 framework, which assigns inflammatory responses to the M1 subset (2, 6, 7, 15). However, the distinctive responses mounted by LPMs and SPMs to LPS stimulation make it difficult to map LPMs and SPMs into the M1/M2 model. Our in vitro stimulation data would suggest that only LPMs should be classified as M1 because LPMs produce NO in response to LPS stimulation whereas SPMs do not. Conversely, our in vivo stimulation data put both LPMs and SPMs into the M1 classification because both produce large amounts of NO in response to LPS. Therefore, the M1/M2 framework does not readily accommodate the SPM and LPM subsets, or vice versa.

Similarly, there is no clear way to retrospectively assign functions established for thioglycolate-stimulated PerC MØ to LPM or SPM. By 4 d after stimulation, very few cells with the typical LPM phenotype are detectable. Because we have shown that LPMs do not differentiate to SPMs or other peritoneal cells (Fig. 7), we conclude broadly that thioglycolate stimulation kills LPMs, forces them to migrate out of PerC, or stimulates them to adhere to the margins of the peritoneum. SPMs, in contrast, flourish in response to thioglycolate stimulation and become the dominant PerC MØ subset, in part because of the loss of LPMs but mainly because of the influx of blood monocytes and the differentiation of these cells to SPMs (Fig. 8). Under conditions used in previous studies, however, the shift we observe may not have been as dramatic. Further, it is important to recognize that functional activities that were detected could also be a result of other remaining (i.e., resident) or elicited cells in PerC (Fig. S1). Thus, at present, one can at best guess that most of the functions previously attributed to thioglycolate-elicited "macrophages" largely reflect SPM functional activity.

In any event, the changes induced by LPS and thioglycolate stimulation open a window on the origins of SPMs. These stimulations result in the rapid entry of a sizable population of blood monocytes (Ly-6C^{hi}MHC-II^{-}) into PerC and the gradual differentiation of these cells to cells that express the typical SPM phenotype (Ly-6C^{-}MHC-II^{hi}; Fig. 8). This developmental process appears to continually be occurring at low levels in unstimulated PerC (Figs. 6 and 8). However, without the severe disruption of the peritoneal economy by LPS or thioglycolate stimulation, it would have been difficult to detect this apparently continuous developmental process.

These findings extend the model presented by Geissmann and coworkers (8, 9, 16), which subdivides blood monocytes into two subsets: an Ly-6C^{-} "resident monocyte" subset that ultimately differentiates to resident tissue MØ and an Ly-6C^{hi} "inflammatory monocyte" subset that infiltrates tissues following inflammatory stimuli. Consistent with this model, we show that Ly-6C^{hi} blood monocytes infiltrate PerC after inflammatory stimulation but, importantly, we add that this infiltrating subset contains the progenitors for SPMs, which are appropriately defined as resident PerC MØ. Ly-6C^{-} monocytes can also enter PerC and replenish SPMs under some conditions (16). However, our findings clearly indicate that inflammation induced by LPS or thioglycolate stimulation induces the infiltration of Ly-6C^{hi}

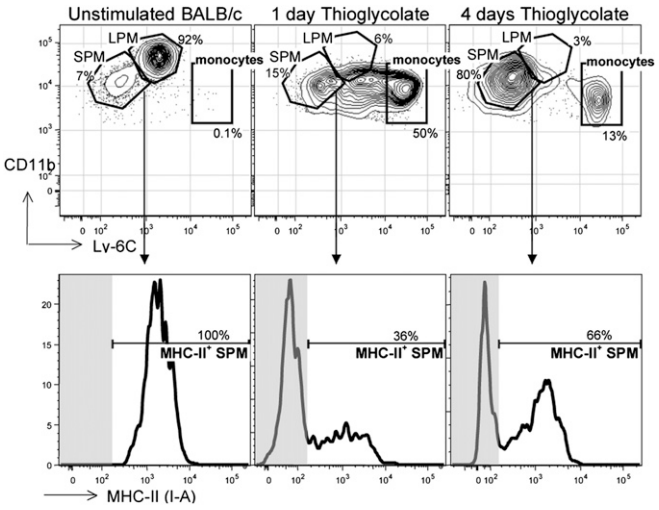

Fig. 8. Thioglycolate stimulation dramatically changes the SPM:LPM ratio. BALB/c mice were injected i.p. with 1 mL of thioglycolate broth. After 1 d and 4 d, PerC cells were analyzed for the presence of myeloid cells. SPMs and LPMs were identified as in Fig. 1. Neutrophils and eosinophils were best gated out from this analysis by using the gating strategy shown in Fig. S1.

inflammatory blood monocytes that differentiate to SPMs that are phenotypically indistinguishable (currently) from typical resident SPMs in PerC from unstimulated animals.

In contrast, our data do not provide insights into the origins of the resident LPM subset in PerC. It could be replenished from the large pool of SPMs present in the stimulated PerC, but we have no data to indicate that this is so.

Conversely, our demonstration that approximately half of the SPMs in PerC express the L-selectin CD62L (Fig. S3) supports the idea that appropriately stimulated SPMs may migrate to lymph nodes and serve as antigen-presenting cells. Indeed, a recent study (17) shows that i.p. immunization with antigen plus alum results in the migration of myeloid cells to lymph nodes, where they differentiate to DCs that can participate in stimulating antibody responses. As the phenotype of the migrating cells was shown to be similar to the SPM phenotype, we suggest that SPMs are sensitive to alum immunization and respond by migrating to locations where they can trigger immune responses.

Materials and Methods

Mice and Tissue Preparation. BALB/c, C57BL/6, 129/S6, FVB/N, SJL/J, and RAG1-KO mice, 6 to 8 weeks old, were purchased from Jackson Labs or bred locally. All mice were maintained at the Stanford Medical School Animal Care Facility. All experiments were conducted with institutional animal care and use committee approval. Peritoneal cells were harvested by injecting 7 mL of staining medium (deficient RPMI plus 3% newborn calf serum) into PerC. Spleen and lymph nodes were disrupted and resuspended to obtain single cell suspensions. Mouse blood was drawn into heparin-containing PBS solution. All cell samples were resuspended at 25×10^6 cells/mL using custom RPMI 1640 medium deficient in biotin, L-glutamine, phenol red, riboflavin, and sodium bicarbonate (Invitrogen).

FACS. Cell suspensions were preincubated with anti–CD16/CD32 mAb to block FcγRII/III receptors and stained on ice for 15 min. with the following fluorochrome-conjugated mAb in an 11-color staining combination: FITC-labeled anti-Ly-6C (AL-21), F4/80 (BM8), CD80 (16-10A1), or CD49b (DX5); PE-labeled anti–I-A^d (AMS-32.1), H-$2K^d$ (SF1-1.1), CD40 (3/23), TLR4-MD-2 (MTS510), or CD49b (DX5); PECy5-labeled anti-CD5 (53–7.3); PECy5.5-labeled anti-CD19 (1D3) or CD11c (N418); PECy7-labeled anti–Gr-1 (RB6-8C5) or IgM (331); APC-labeled anti-B220 (RA3–6B2), CD86 (GL-1), CD117 (c-kit 2B8) or AA4.1; Alexa700-labeled anti-IgD (11-26); APCCy7-labeled anti-CD11b (M1/70); Pacific Blue–labeled anti-F4/80 (BM8) or Gr-1 (RB6-8C5) and biotin-labeled anti-CD11c (HL3). Cells were then washed and stained again on ice for 15 min with streptavidin Qdot 605 (Invitrogen) to reveal biotin-coupled antibodies. Antibodies were either purchased (Invitrogen and BD Pharmingen) or conjugated in our laboratory. After washing, stained cells were resuspended in 10 μg/mL propidium iodide, to exclude dead (i.e., propidium iodide–negative) cells. Cells were analyzed and sorted on Stanford FACS facility instruments (Becton Dickinson LSRII or FACSAria). Data were collected for 0.2 to 1×10^6 cells. Staining protocols were designed with CytoGenie software (WoodSideLogic); data were analyzed with FlowJo software (TreeStar). To distinguish autofluorescent cells from cells expressing low levels of individual surface markers, we established upper thresholds for autofluorescence by staining samples with fluorescence-minus-one control stain sets (18, 19) in which a reagent for a channel of interest is omitted.

In Vitro and in Vivo Stimulation. In vitro, 10^6 PerC cells were cultured with and without 1μg/mL of LPS (*E. coli* 055:B5; Sigma) in a final volume of 500 μL of RPMI-1640 plus 10% FCS. Cells were incubated at physiologic oxygen levels (5% O_2) for indicated times. For NO measurement, cells were resuspended in 1mL of medium containing 0.1% probenecid (pH 7.4) and maintained subsequently in this medium. Cells were incubated in the presence of 1 μM of 4-amino-5-methylamino-2′,7′-difluorescein (DAF-FM) diacetate (Molecular Probes) at room temperature for 30 min and stained and analyzed by flow cytometry. In vivo, 1 mL of thioglycolate broth or 5 μg or 10 μg of LPS (in 200 μL of PBS solution) were injected i.p. At indicated times, PerC was harvested, stained, and analyzed.

In Vivo Phagocytosis Assay. *E. coli* (K-12) bacteria (5×10^6) expressing GFP were taken from overnight culture and resuspended in 500 μL of PBS solution. The GFP^+ bacteria were then injected into the PerC of BALB/c mice. After 2 h, total PerCs were harvested, stained, and analyzed for the presence of GFP^+ bacteria.

Confocal Microscopy. GFP^+ SPMs and LPMs were FACS-sorted directly onto a coverslip, fixed in 4% formalin for 15 min, washed in PBS solution, and air-dried. Finally, the coverslip was mounted to the slide using ProLong Gold antifade reagent containing DAPI (Invitrogen; Molecular Probes). The images were collected on a microscope (Optiphot-2; Nikon) attached to a confocal laser scanning (MRC1024; Bio-Rad) by using LaserSharp software (Bio-Rad). To identify extracellular bacteria, we used primary rabbit polyclonal anti-LPS followed by Alexa594-labeled goat anti-rabbit antibodies. Thus, bacteria that have remained attached on the cell membrane (not internalized) appear red. Internalized bacteria were visualized as green. The blue staining shows phalloidin coupled to Alexa647, which stains actin and gives the outline of the cell cytoplasm. Volocity 3.0 software (Improvision) was used to format and then merge the green (GFP), red (Alexa594), and blue (Alexa647) images. To measure individual cell size (Fig. 2), differential interference contrast images were acquired by confocal microscopy (LSM 510 META; Zeiss) with a ×63 Plan Apochromat objective lens (NA 1.4). Cell diameter was determined using Zeiss software.

ACKNOWLEDGMENTS. We thank Megan Phillips for outstanding technical help, Thomas Henry for bacterial killing by MØ; Lauren Higdon for MHC staining; Robert Axtell for supportive discussion; P. Sadate-Ngatchou, N. Zimmerman, K. Atkuri, and Y. Gernez for critical reading of this manuscript; and John Mantovani and Claudia Weber for administrative support. This work was supported by National Institutes of Health Grant AI076434.

1. Taylor PR, Brown GD, Geldhof AB, Martinez-Pomares L, Gordon S (2003) Pattern recognition receptors and differentiation antigens define murine myeloid cell heterogeneity ex vivo. *Eur J Immunol* 33:2090–2097.
2. Gordon S, Taylor PR (2005) Monocyte and macrophage heterogeneity. *Nat Rev Immunol* 5:953–964.
3. Taylor PR, et al. (2005) Macrophage receptors and immune recognition. *Annu Rev Immunol* 23:901–944.
4. Cohn ZA (1968) The structure and function of monocytes and macrophages. *Adv Immunol* 9:163–214.
5. van Furth R (1985) Monocyte production during inflammation. *Comp Immunol Microbiol Infect Dis* 8:205–211.
6. Mills CD, Kincaid K, Alt JM, Heilman MJ, Hill AM (2000) M-1/M-2 macrophages and the Th1/Th2 paradigm. *J Immunol* 164:6166–6173.
7. Mantovani A, et al. (2004) The chemokine system in diverse forms of macrophage activation and polarization. *Trends Immunol* 25:677–686.
8. Geissmann F, Jung S, Littman DR (2003) Blood monocytes consist of two principal subsets with distinct migratory properties. *Immunity* 19:71–82.
9. Geissmann F, et al. (2008) Blood monocytes: distinct subsets, how they relate to dendritic cells, and their possible roles in the regulation of T-cell responses. *Immunol Cell Biol* 86:398–408.
10. Steinman RM, Moberg CL (1994) Zanvil Alexander Cohn 1926-1993. *J Exp Med* 179:1–30.
11. Bogdan C, Schleicher U (2006) Production of interferon-gamma by myeloid cells—fact or fancy? *Trends Immunol* 27:282–290.
12. Cohn ZA (1978) Activation of mononuclear phagocytes: fact, fancy, and future. *J Immunol* 121:813–816.
13. Lagasse E, Weissman IL (1996) Flow cytometric identification of murine neutrophils and monocytes. *J Immunol Methods* 197:139–150.
14. Takahashi M, Galligan C, Tessarollo L, Yoshimura T (2009) Monocyte chemoattractant protein-1 (MCP-1), not MCP-3, is the primary chemokine required for monocyte recruitment in mouse peritonitis induced with thioglycollate or zymosan A. *J Immunol* 183:3463–3471.
15. Martinez FO, Helming L, Gordon S (2009) Alternative activation of macrophages: an immunologic functional perspective. *Annu Rev Immunol* 27:451–483.
16. Auffray C, et al. (2007) Monitoring of blood vessels and tissues by a population of monocytes with patrolling behavior. *Science* 317:666–670.
17. Kool M, et al. (2008) Alum adjuvant boosts adaptive immunity by inducing uric acid and activating inflammatory dendritic cells. *J Exp Med* 205:869–882.
18. Roederer M (2001) Spectral compensation for flow cytometry: visualization artifacts, limitations, and caveats. *Cytometry* 45:194–205.
19. Herzenberg LA, Tung J, Moore WA, Herzenberg LA, Parks DR (2006) Interpreting flow cytometry data: a guide for the perplexed. *Nat Immunol* 7:681–685.

Supporting Information

Bou Ghosn et al. 10.1073/pnas.0915000107

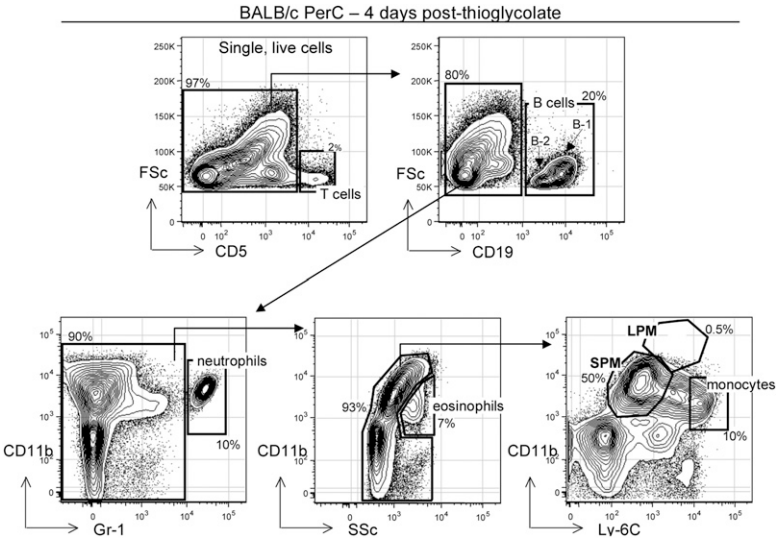

Fig. S1. PerC cells harvested at d 4 after thioglycolate stimulation contain SPMs and a variety of other leukocytes. BALB/c mice were injected i.p. with 1 mL of thioglycolate broth. After 4 d, PerC cells were harvested, stained, and analyzed for the presence of immune cells subsets.

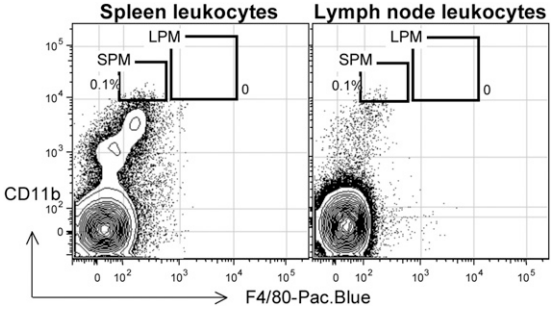

Fig. S2. SPMs and LPMs are virtually absent in mouse spleen and lymph nodes. Cells from spleen and lymph node from unstimulated BALB/c mice were harvested, stained, and analyzed for the presence of SPM and LPM, identified as in Fig. 1 in the main text. Data shown for cells collected from mesenteric lymph node are also representative of data obtained for inguinal lymph nodes.

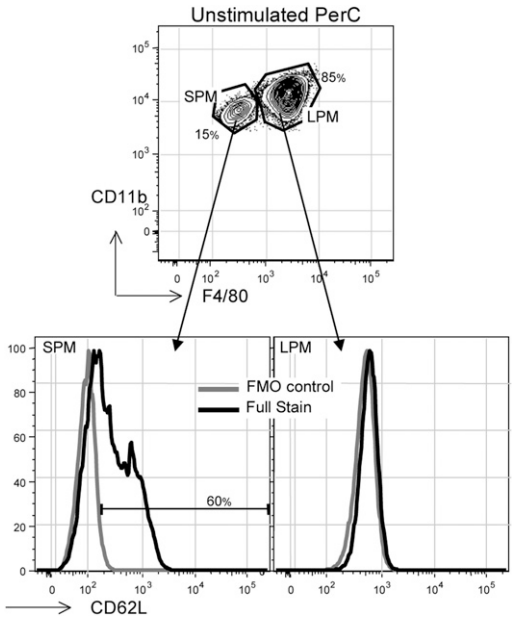

Fig. S3. CD62L is expressed on approximately half of the SPM population. SPMs and LPMs were identified as in Fig. 1 in the main text and analyzed for the surface expression of CD62L.

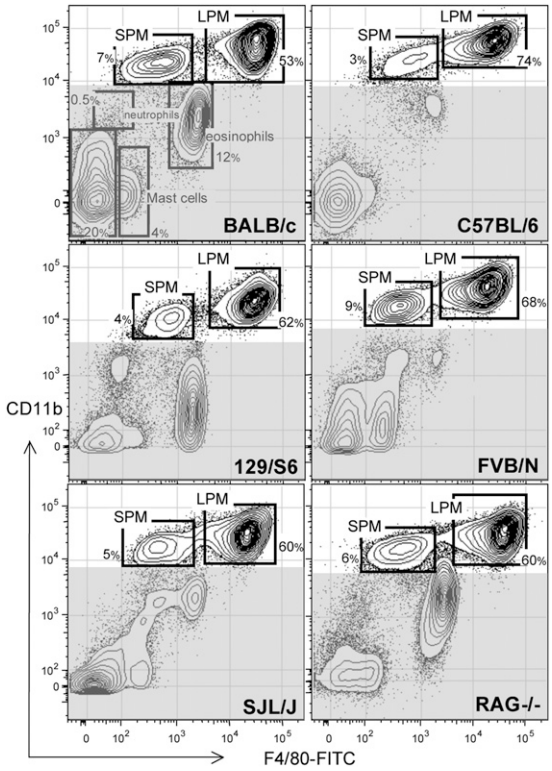

Fig. S4. SPMs and LPMs are present in a variety of mouse strains. PerC cells from unstimulated BALB/c, C57BL/6, 129/S6, FVB/N, SJL/J, and RAG$^{-/-}$ mice were harvested, stained, and analyzed for the presence of SPMs and LPMs. SPMs and LPMs were identified as in Fig. 1 in the main text. Data shown are representative of at least three experiments.

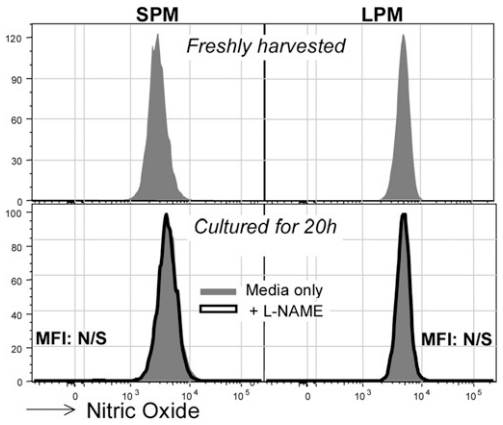

Fig. S5. Culturing PerC for 20 h in the absence of LPS does not induce intracellular NO production in PerC MØ. SPMs cultured for 20 h without LPS (*Lower*) show a slight increase in DAF-FM staining relative to SPMs in freshly harvested PerC (*Upper*). To determine whether this increase is a result of spontaneous production of NO (or to "nonspecific" DAF-FM staining), we compared DAF-FM staining of 10^6 PerC cultured (as in Fig. 5) for 20 h (*Lower*) in the presence (black histogram) or absence (gray histogram) of 1.5 mM L-NAME, a standard inhibitor of NO production. SPMs and LPMs were identified and gated as in Fig. 1 in the main text. N/S, not significant.